1. Introduction

Around 90% of the US population currently relies on centralized water supply systems, which are often characterized as infrastructure with distribution networks that provide service to an entire city or region (Dieter et al. 2018). With the benefit of economies-of-scale, these centralized systems can supply sufficient quantities of easily accessed, high-quality potable water with a relatively low cost to the consumers (Hunter et al. 2010). Nevertheless, management of these systems has become increasingly challenging. In the US, many crucial water conveyance pipes were installed over 100 years ago, while the total expected lifespan of the pipes is generally between 75 and 100 years (ASCE 2017). The country has fallen behind on repairing or replacing aged water systems. There are an estimated 240,000 water main breaks per year, resulting in losses of around six billion gallons of treated water per day (ASCE 2017). An estimated investment of $250 billion over the next 30 years is needed to replace the aged water pipes and fixtures (AWWA 2001). Additionally, the centralized water supply scheme can have high vulnerability and lack adaptability to the increasingly common natural (e.g., droughts and flooding) and manmade (e.g., terrorist attacks) threats. On the other hand, decentralized water supply systems have been developed and increasingly integrated within the centralized network. Decentralized or distributed systems are smaller-scale dispersed facilities that are located near or at the point of use (JFW 2014). They can either function independently or remain connected to a centralized system (JFW 2014). Rainwater harvesting (RWH) and greywater recycling (GWR) systems are currently the two most widely investigated/implemented decentralized water systems (López Zavala et al. 2016). Decentralized systems are often touted as money- and energy-saving investments; however, poorly sized or sited systems can lead to an increased cost for the consumer and a net energy loss (Wang and Zimmerman 2015). A holistic understanding of how the decentralized water systems can be integrated on a city-scale to improve sustainability and resiliency is hence imperative.

Over the last decade, life cycle assessment (LCA) and life cycle cost assessment (LCCA) have been increasingly applied for assessing RWH and GWR systems, although much uncertainty still exists as whether the decentralized systems can result in positive cost or energy savings. Many of these studies

adopted a case study approach that focused on specific building settings (e.g., Morales-Pinzón et al. 2015, Wang and Zimmerman 2015), but did not consider the influence of adoption patterns on a city scale. They commonly suggested that RWH or GWR systems with a higher service population or population density are more likely to achieve cost or energy savings (e.g., Godskesen et al. 2011, Jeong et al. 2016, Memon et al. 2007, Newman et al. 2014a, Wanjiru and Xia 2017, Ward et al. 2012). Only a few of these studies have considered the avoided treatment and pumping needs at the centralized plants as a result of the adoption (Angrill et al. 2012, Ghimire et al. 2014, Godskesen et al. 2011, Newman et al. 2014b, Ward et al. 2012). Of these that did consider the avoided treatment and pumping needs, findings vary significantly depending on the design of the decentralized systems and the system boundary that has been included in the analysis. None of these studies, however, considered the influence of household location within the context of the existing centralized network on the avoided pumping needs.

Very few studies have examined the influence of integrating decentralized water systems into the existing centralized networks on a city scale. Matteo et al. (2017) investigated the optimized spatial distribution of RWH system adoptions based upon supply volume, water quality improvement, and life cycle cost. They found integrating RWH systems into the centralized network can improve the reliability of the water supply, but there is a tradeoff between reliability and cost. Similarly, Penn et al. (2013) optimized the spatial distribution of homes with GWR systems in a neighborhood to minimize life cycle energy cost and wastewater outflow using hydrodynamic modeling. They found the optimal amount of greywater water usage was highly related to the spatial location of the households. This study, however, did not include a full life cycle assessment. Neither studies, however, investigated the optimized sizing of the decentralized systems. Kavvada et al. (2016), on the other hand, investigated the optimal size and locations of shared decentralized water reuse systems in San Francisco, California. Optimal distribution was based on life cycle cost, energy and greenhouse-gas emissions which were determined by home elevation, population density, and road network analysis. This study determined that savings were more sensitive to spatial determinants for decentralized systems than their size or scale. One recent study investigated the optimal integration of

GWR and RWH systems at a regional scale based upon water volume and cost savings (Hargreaves et al. 2019). However, life cycle energy savings as well as the avoided treatment and pumping needs from the centralized plants were not investigated.

Most of the previous studies often investigate RWH and GWR systems separately, making their comparisons difficult. Ghisi, Rupp, and Triska (2014) applied RWH, GWR, and other potable water saving methods to a single school building in Brazil to examine the energy and cost outcomes. The RWH system was found to have a shorter payback period compared with the GWR system. However, the study used fixed flow rates and sizes to model the systems over the systems' life span. On the other hand, Chang, Lee, and Yoon (2017) looked at the operation phases of GWR, RWH, as well as a typical centralized plant in South Korea to compare their energy consumptions. The GWR system was determined to be superior than both the RWH and the centralized water supply primarily due to the reduced amount of wastewater that needs to be treated. The completely different recommendations provided by the two studies are likely a result of the varied climate, building, and system settings that have been considered. This suggests the importance of developing models that can be easily generalized for different decentralized system applications.

Our study combines LCA and LCCA with system dynamics modeling, tank size optimization, and spatial analysis. This model gives individual households of varying sizes and characteristics an optimally sized greywater or rainwater system based upon its life cycle cost and energy expenditure. RWH and GWR systems were selected for this study due to their common household applications for onsite non-potable collection and reuse. Areas in a city that can benefit most from decentralized system integration were then investigated. Boston, MA was selected as a study site given its expected population growth and aged water and wastewater infrastructure (Bowen et al. 2019). Our model aims to provide communities a tool that informs the feasibility of adopting decentralized systems based on energy and costs as well as to assist decision-making in future water infrastructure management policies.

2. Methodology

Figure 1 illustrates the overall process of the modeling effort conducted in this study. Two system dynamics models, one for RWH and one for GWR, were first developed to simulate the daily water balance based upon the supply of rainwater or greywater, the non-potable water demand, and the available space in the storage tanks (Section 2.1). LCCA and LCA were then conducted to calculate life cycle cost and energy savings that can be achieved through the decentralized system installations considering their influences on the centralized drinking water treatment plant (DWTP) and the wastewater treatment plant (WWTP; Sections 2.2 and 2.3). These savings were then optimized for each individual residential household in Boston, MA to identify the scientifically optimal locations of decentralized system installations (Section 2.4). All models were developed using the open sourced Python 3.7. A sensitivity analysis was performed to investigate the uncertainties related to key model assumptions (Section 2.5).

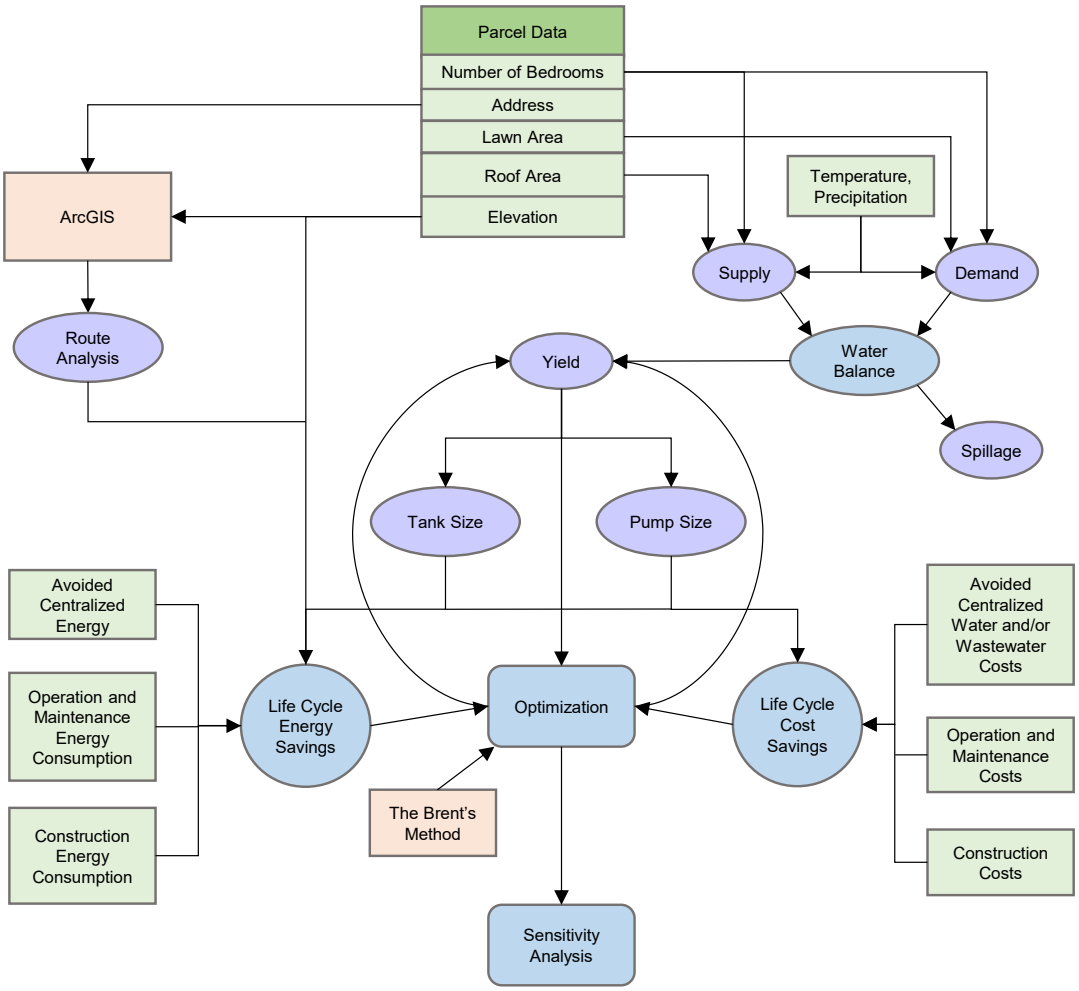

Figure 1 A schematic of the modeling framework applied in the current study

RWH systems store rain that falls on a specific collection area. For this study, residential rooftops were the collection area for each individual system. Rainwater falls on the roof, flows by gravity to gutters, passes through a filter to remove solids, and accumulates in a storage tank at ground level (Figure 2(a)). GWR systems collect water that has already been used in a household for reuse with minimal treatment. Water from sinks, showers, and washing machines is collected in a storage tank (Figure 2(b)). Both the collected rainwater and greywater is used for non-potable uses including toilet flushing and lawn irrigation (Dixon et al. 2000, Hamilton et al. 2017), which reduces the need for having high-quality water in the storage tank (Gwenzi et al. 2015).

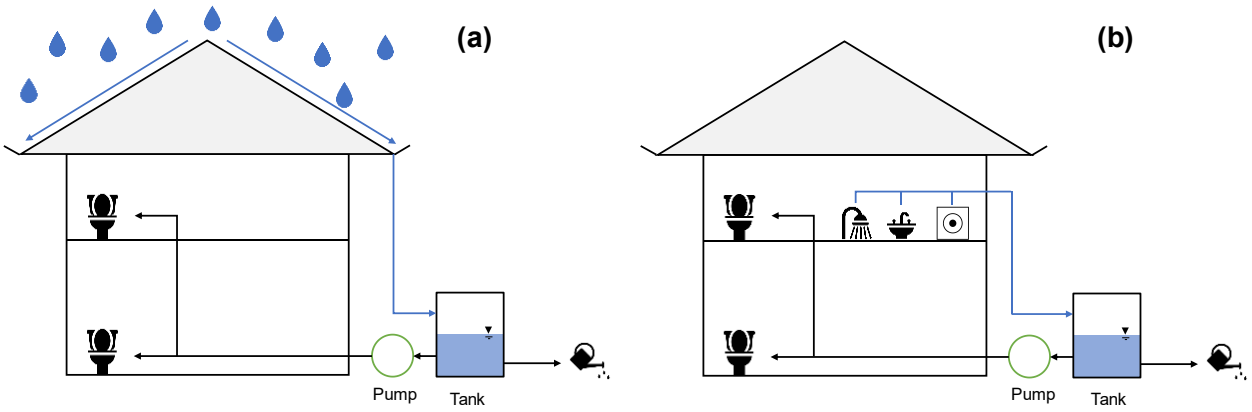

Figure 2 A schematic of the rainwater harvesting (a) and the greywater recycling (b) systems investigated in the current study

Information for the households analyzed in the study was from the City of Boston's open-sourced GIS data portal (Maps 2019). Particularly, the 2016 tax parcel dataset was used to obtain key attributes, including building type, street name and number, living area, number of floors, number of bedrooms, parcel square footage, average elevation, building type, and distance from the treatment plants (COB 2019). Out of the over 160,000 property parcels included within the dataset, only residential buildings were included in the analysis. All commercial buildings as well as any buildings that did not have bathrooms and bedrooms were omitted, which reduced the data size significantly to around 68,000. Apartment units that belong to the same building were combined by matching their street addresses, which allows us to investigate decentralized system installations on a building basis.

2.1 Water Balance Model

2.1.1 Rainwater and Greywater Supply, Yield, and Storage

The dynamic portion of the model stems from rainwater and greywater supply and demand changing daily. For both systems, the yield-after-spillage method was used, meaning excess rainwater or greywater supply beyond the storage capacity will first be spilled. The remaining water in the tank will then be used for meeting the demand. Yield refers to the amount of demand that is met by the available rainwater or

121 greywater volume in storage. This relatively conservative algorithm has been commonly used to simulate
122 RWH models (Hanson et al. 2009, Wang and Zimmerman 2015). In this study, this excess volume becomes
123 runoff for RWH systems or gets diverted to the sewer for GWR systems. The dynamic equations showing
124 the yield and storage of the tank are shown in Eqs. 1 and 2.
125
126 $$Y_t = \min \begin{cases} S_{t-1} \\ D_t \end{cases} \qquad \text{Eq. 1}$$
127
128 $$S_t = \max \begin{cases} T - Y_{t-1} \\ 0 \end{cases} \qquad \text{Eq. 2}$$
129
130 where Y_t is yield on day *t*, m³, S_{t-1} is the volume of water available in the tank from the previous day, *t-1*,
131 m³; T is tank size, m³; and, D_t is demand on day *t*, m³.
132
133 Rainwater supply has an intermittent nature. The total rainfall volume sent to the RWH system each day
134 was calculated using Eq. 3.
135
136 $$S_{RW,t} = \min \begin{cases} RA \times P_t \times C_R \\ T - S_t \end{cases} \qquad \text{Eq. 3}$$
137
138 where $S_{RW,t}$ is the rainfall collected in the tank on day *t*, m³; RA is the roof area, m², assumed to be the
139 same as the buildings' footprint; P_t is the amount of precipitation on day *t*, m; C_R is the roof runoff
140 coefficient, which was assumed to be 0.9 (Wang and Zimmerman 2015); and, S_t is the amount of water
141 volume available in the tank on day *t*, m³. Particularly, daily precipitation data between 1988-2018 for
142 Boston, MA was acquired from the Logan Airport gauge (NOAA 2019) to simulate rainwater supply over
143 the assumed 30-year life span of RWH systems (Morales-Pinzón et al. 2015).
144

GWR systems have a consistent daily supply dependent on occupancy. The total greywater volume sent to the GWR system each day was calculated using Eq. 4.

$$S_{GW,t} = \min \begin{cases} N \times OC \times (SH_t + L_t + SU_t) \\ T - S_t \end{cases} \quad \text{Eq. 4}$$

Where $S_{GW,t}$ is the daily greywater collected in the tank, m³; N is the number of bedrooms; OC is the average occupancy per bedroom calculated by dividing the Greater Boston area population (USCB 2019) by the total number of bedrooms in the residential buildings in this area, 2.47 persons/bedroom; SH_t is the shower water usage per person per day, 0.065 m³/person/day (USGS 2019); L_t is laundry water usage per person per day, 0.018 m³/person/day (USGS 2019); and SU_t the sink water usage per person per day, 0.023 m³/person/day (USGS 2019).

2.2.2 Rainwater and Greywater Demand

For this study, the non-potable uses are toilet flushing and lawn irrigation for both system types. The daily water use by toilet flushing was determined by daily flushing usage, or fixture rate, 0.072 m³ per person per day (Dieter et al. 2018) and the occupancy. Lawn irrigation was assumed to only occur between May and September and on days when there is no precipitation (Steffen et al. 2013). On days when lawn irrigation is needed, volume was determined using Eq. 5 (Kjelgren et al. 2016). All unmet demand was assumed to be supplemented by the centralized DWTP.

$$D_{I,t} = \begin{cases} E \times PF \times LA/(EF \times 1000) & if \quad P_t = 0, t \in IP \\ 0 & if \quad otherwise \end{cases} \quad \text{Eq. 5}$$

Where $D_{I,t}$ is irrigation demand, m³; *IP* indicates the period in which lawn irrigation is typically applied, May to September; *E* is the evapotranspiration rate, which was assumed to be 2.79 mm for Boston during *IP* period (NRCC 2020); *LA* is the lawn area, m², which was estimated by subtracting the footprint of the

building from the land parcel; *EF* is the irrigation efficiency, which was assumed to be 50% (EPA 2003); and *PF* is the plant factor, which was assumed to be 0.8 (NRCC 2020, Romero and Dukes 2008).

2.2 Life Cycle Cost Model

The life cycle saving of a decentralized system depends on the capital, operation, and maintenance costs as well as the achievable economic savings over a 30-year life span. A net present value method was adopted which discounts all future costs back to the 2018-dollar value using an annual discount rate of 3%.

2.2.1 Capital Cost

Capital costs include construction and installation costs, while the construction cost consists of the pump cost, tank cost, and design cost. Pump cost was estimated based upon its horsepower using Eqs. 6-8. There was a minimum horsepower requirement of 0.5 due to typical pump sizes. Simultaneity factors were used to adjust the required pump horsepower based upon the fact that it is unlikely for all fixtures to operate simultaneously. Simultaneity factors are tiered values assigned based upon a building's toilet flushing demand (INTEWA 2020). See the Supporting Information for detailed values of the simultaneity factors used in this study.

$$PC = -9.1053 \times P_h^2 + 341.42 \times P_h + 463.63 \qquad \text{Eq. 6}$$

$$P_h = \max\begin{cases} 0.5 \\ F \times NF \times W \times f \times H_{req}/(PE \times k) \end{cases} \qquad \text{Eq. 7}$$

$$H_{req} = h_p + h_e + h_f \qquad \text{Eq. 8}$$

Where PC is pump cost, \$2018 USD; P_h is pump required hydraulic power, hp; F is fixture water flow rate; 0.000252 m³/s; NF is number of fixtures in the building, which was estimated to be occupancy divided by

2; W is water density, 1000 kg/ m³; f simultaneity factor; H_{req} is pump required head, m; PE is pump efficiency, which was assumed to be 0.5; k is a conversion factor, 75 kg·m/s per hp; h_p is operation head for a fixture, assumed to be 14 m (Jones M 2020); h_e is elevation head calculated as building height minus 3 m, m; h_f is friction loss, assumed to be 0.2 times of the approximate pipeline length, m. Pipeline length was estimated based upon building height and building area. See the Supporting Information for a more detailed description of the pipeline length estimation.

The tank cost was a function of tank size calculated using Eq. 9 (WERF 2009). Tanks were assumed to be made of plastic materials. Installation cost was assumed to be 60% of the tank cost (WERF 2009), while the design cost was assumed to be 8% of the tank and pump costs (WERF 2009).

$$TC = (1.896 \times T^2 + 91.438 \times T + 261.9) \times \alpha \qquad \text{Eq. 9}$$

Where TC is tank cost, \$2009 USD; T is tank size, m³; and α is a conversion factor for adjusting \$2009 USD to \$2018 USD based on the historical average annual Consumer Price Index data (USBLS 2020).

2.2.2 Operation and Maintenance Cost

The operation cost was calculated based on the pumping energy for operating the decentralized systems based on Eqs 10-11. It was assumed that only the water for toilet flushing needs to be pumped upwards, while irrigation is gravity-fed. An indoor use ratio was used to indicate the proportion of rainwater or greywater that is used for toilet flushing out of the total yield on a particular day.

$$PEC_t = Y_t \times IU_t \times g \times H_{req} \times EP/(PE \times 3600) \qquad \text{Eq. 10}$$

Where PEC_t is daily pumping energy cost, \$; Y_t is yield on day t, m³; IU_t is indoor use ratio on day t, dimensionless; g is gravity acceleration, 9.81 m/s^2; EP is the electricity price, which was assumed to be \$0.216/kWh for Boston (USBLS 2020).

Maintenance cost was set at \$100 annually, which falls within the suggested range by various literature sources (USEPA 2013, WERF 2009). Maintenance of the system is required to ensure the tank and filter are in proper working order and unobstructed by clogs or failing equipment.

2.2.3 Cost Benefit

RWH systems can reduce potable water purchases from the centralized DWTP. GWR systems can reduce both potable water purchases and wastewater generations. Both benefits reduce the customer's monthly water bills. Boston's 2018 water rates were used for the simulation, with \$1.82 per m³ for purchased potable water and \$2.41 per m³ for sewer (BWSC 2019). For GWR systems, the combined savings per reused unit of greywater was \$4.23 per m³. Although wastewater is generally charged based on drinking water usage in real life given a separate sewer meter is typically not installed, landlords in Massachusetts are permitted to implement individual sewer meters to accurately measure sewerage. The price elasticity of demand was not considered because decentralized system adoption is considered to offset potential future increases in drinking water demand and wastewater generation due to population and economic growth.

2.3 Life Cycle Energy Model

The life cycle energy model considers the energy expenditure of installing and operating an RWH or GWR system and the avoided energy for pumping and treatment at the centralized DWTP and the WWTP. RWH systems affect the pumping and treatment energy use in the centralized DWTP, while the GWR systems affect the energy use in both the DWTP and the WWTP.

2.3.1 Avoided Pumping Energy

The avoided pumping energy from the DWTP was estimated using Eqs. 10-14. Wastewater was assumed to be transferred to the WWTP by gravity, and hence the avoided pumping energy from the WWTP was not considered.

$$PM_t = Y_t \times W \times g \times TH/(CP \times \beta) \quad \text{Eq. 10}$$

$$TH = \begin{cases} FL + \Delta E + OP + VH & if \quad FL + \Delta E + OP + VH > 0 \\ 0 & if \quad FL + \Delta E + OP + VH \leq 0 \end{cases} \quad \text{Eq. 11}$$

$$FL = FC \times DP \quad \text{Eq. 12}$$

$$\Delta E = HE - PE \quad \text{Eq. 13}$$

$$VH = 0.5 \times V^2/g \quad \text{Eq. 14}$$

where PM is centralized pumping energy savings on day *t*, kWh; *TH* is total head, m; *CP* is the centralized DWTP pumping efficiency, which was assumed to be 70%; β is a conversion factor, 3.6×10^6 Joule/kWh; FL is friction loss, m; ΔE is the elevation head, m; OP is operating head, which was assumed be 49.2 m in order to meet the maximum daily demand and the requirement for fire protection (MWRA 2006); *VH* is the velocity head or the dynamic pressure, m; FC is friction loss coefficient, estimated to be 8 m/km, based on approximate pipe material and diameter (Ghorbanian et al. 2016, NRCNA 2006); DP is the minimum piping distance from each building to the DWTP, km; HE is household elevation, m, PE is the elevation of the DWTP, m; and V is water velocity in the pipe, assumed to be 2 m/s (Brière 2014). Particularly, *DP* was estimated based upon Boston's road network, assuming water pipes are located along the roads (Kavvada et al. 2016). A road network dataset was collected from Boston's GIS data portal (COB 2019, Maps 2019). Approximate piping distance between the households and the DWTP was found using the Network Analyst

toolset in ArcMap 10.6 using the closest facility function (Figure 3). The network was completed by finding the centroid of each tax parcel, determining the closest road to each centroid, and creating a line from the centroid to the road network. The residential buildings, their corresponding data, and the DWTP were placed in the road network layer using the geo-referencing tool and address locators in ArcMap. Elevation of the households and the DWTP was determined using an elevation contours dataset from Boston's GIS data portal (Maps 2019). The elevation of each tax parcel was determined by finding the average elevation spatially across the parcel.

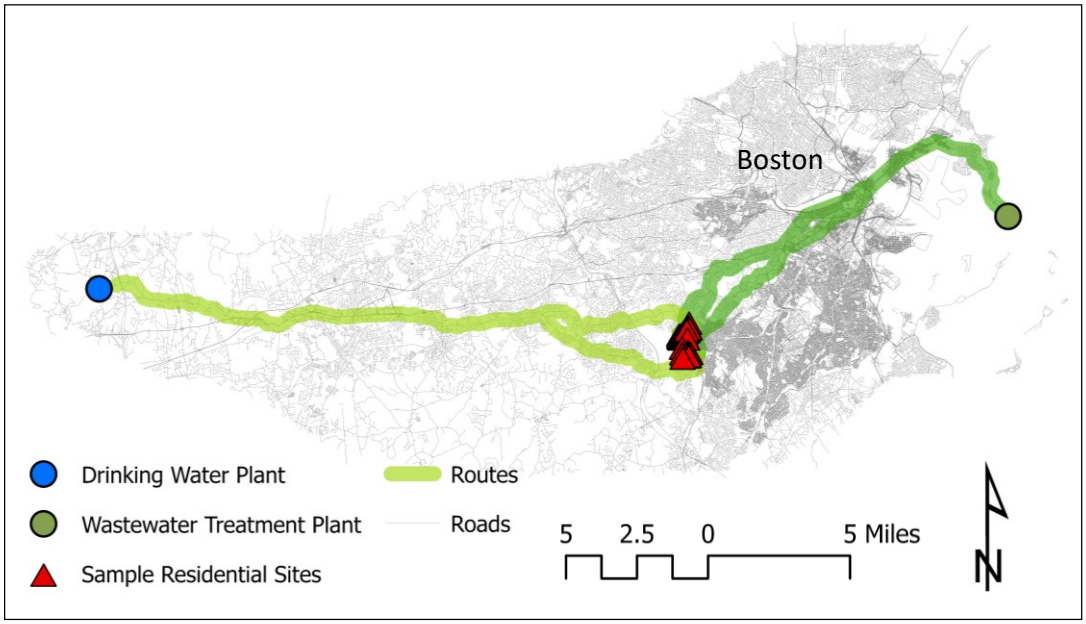

Figure 3 Pipeline network developed based upon the road network in Boston. Routes shown in the map are example routes generated between selected households and the drinking water treatment plant (indicated by the blue dot) and the wastewater treatment plant (indicated by the green dot).

An empirical method was used to calibrate the modeled pumping energy to match the actual pumping energy used by the DWTP. To achieve this, annual total operational energy usages were obtained from the DWTP (i.e., John J. Carroll Water Treatment Plant). Pumping energy was assumed to represent 86% of the DWTP's operational energy based on national average data (EPRI 2002). Accordingly, the actual pumping energy intensity was estimated to be 0.19 MJ/m^3. We then used Eqs. 10-14 to model the pumping energy

saving for an "average" household over 30 years based on average household characteristics obtained from the tax parcel dataset. The average household features 3 floors, 74-meter elevation, 269.4-m^2 living area, 390.2-m^2 land area, and 41.9-km distance from the DWTP, with a 5-m^3 tank installed. A correction factor was then calculated to match the modeled avoided pumping energy intensity to the actual DWTP pumping intensity of 0.19 MJ/m^3. The correction factor was 0.04 for both RWH and GWR systems.

The calibrated pumping energy was then converted to the primary energy form. A conversion factor of 2.26 MJ/MJ was obtained from SimaPro 8.5 by applying the *Cumulative Energy Demand V1.10* method to a data entry named "*Electricity, medium voltage (Abbas et al.)| market group for | Conseq, U*".

2.3.2 Avoided Treatment Energy

The avoided treatment energy was obtained from previous life cycle assessment studies on the John J. Carroll Water Treatment Plant (Mo et al. 2016) and the Deer Island Wastewater Treatment Plant (Khalkhali and Mo 2020). The energy intensity of drinking water treatment was estimated to be 1.62 MJ of primary energy/m^3, while the energy intensity of wastewater treatment was estimated to be 1.68 MJ of primary energy/m^3 (Khalkhali et al. 2018, Mo et al. 2016).

2.3.3 Energy Used for Constructing, Operating, and Maintaining Decentralized Systems

Energy usages for the decentralized systems were calculated for each of the residential households in the Boston tax parcel dataset. Construction energy is a single energy expenditure that accounts for pump manufacturing, tank manufacturing, and installation. These three components were calculated using the Economic Input-Output Life Cycle Assessment (EIO-LCA) web tool (CMU 2018). The "pump and pumping equipment manufacturing" sector was used for calculating the pump manufacturing energy intensity, and the associated embodied energy intensity was 8.49 MJ of primary energy/2002 USD. The "other plastic products manufacturing" sector was used for calculating the tank manufacturing energy intensity, and the embodied energy intensity was 14.8 MJ of primary energy/2002 USD. The "residential

permanent site single- and multi-family structures" sector was used to find the energy intensity of system installation, and its embodied energy intensity was 8.91 MJ of primary energy/2002 USD. Each of these energy intensities was multiplied with their respective cost calculated in Section 2.3.1 to obtain its total energy usage.

The operation energy usage calculated from Eq. 10 was converted to the primary energy form using a factor of 2.26 MJ/MJ. The maintenance energy was also calculated using the EIO-LCA tool. The "other support services" sector was used to find the energy intensity of maintenance, which was 3.72 MJ/2002 USD (CMU 2018). The maintenance energy intensity was then multiplied with the total maintenance cost to obtain the total maintenance energy usage.

2.4 Optimization of Tank Sizes

Tank size was optimized for each household to maximize either net cost or energy savings. The Brent's method was used to select the optimal tank size (Brent 1971). The Brent's method searches for the maximum savings point of each household using the bisection method, secant method, and inverse quadratic interpolation. The bisection method splits the output data in half until it finds the point of interest, in this case the maximum cost or energy savings. To use the Brent's method, scipy.optimize and negative minimized scalar function was coded, with an accuracy range of 0.2 m^3. Since the Brent's method requires bounds to operate within, the maximum possible tank size was assumed to be 40 m^3. Brent's method assumes the function is concave. If the model's output does not result in a concave function, the computed solution may be suboptimal. However, in our model tests on randomly selected households, we found all of the cost and energy results as a function of tank size are concave. Two optimal sizes were calculated for each system, one based on the highest life cycle cost savings and one based on the highest life cycle energy savings.

2.5 Sensitivity Analysis

To evaluate which variables had the greatest effect on the cost and energy outcomes, a sensitivity analysis was conducted. All the constant input variables were varied and tested in the sensitivity analysis for the average household described in Section 2.4.1 over its life span. The tested variables include height per floor, electricity price, pump efficiency, water price, fixture rate, lawn condition, irrigation efficiency, water velocity in pipes, discount rate, laundry loads, shower flow, sink flow, occupancy per bedroom, friction loss coefficient, central pump efficiency, operation pressure, maintenance energy intensity, pump embodied energy, tank embodied energy, installation energy intensity, installation cost, annual maintenance cost, evapotranspiration rate, and plant factor. Input variables were changed by ±25% and ±50% to represent a reasonable range of possible values. To determine the variables' influence on the outcomes, Eq. 14 was used to create a sensitivity index (Song et al. 2019). Variables were considered highly sensitive if their indices were greater than one.

$$SI = \frac{\frac{CO - OO}{OO}}{\frac{CI - OI}{OI}} \quad \text{Eq. 15}$$

where SI is sensitivity index, CO is the changed output value, OO is the original output value, CI is changed input value, and OI is original input.

3. Results and Discussion

This section describes the spatial patterns of life cycle cost and energy savings under city-scale residential adoptions of RWH (Section 3.1) and GWR (Section 3.2) systems in the testbed area of Boston. A comparison of the optimal spatial adoption patterns of the RWH and GWR systems was made and its implications were discussed (Section 3.3). Lastly, findings from the sensitivity analysis were presented and discussed (Section 3.4). Figure 4 provides an overview of all neighborhoods within the City of Boston to assist the spatial distribution discussions in the following sections. Additional information related to the spatial distributions of household characteristics was provided in Figure S-1 of the support information.

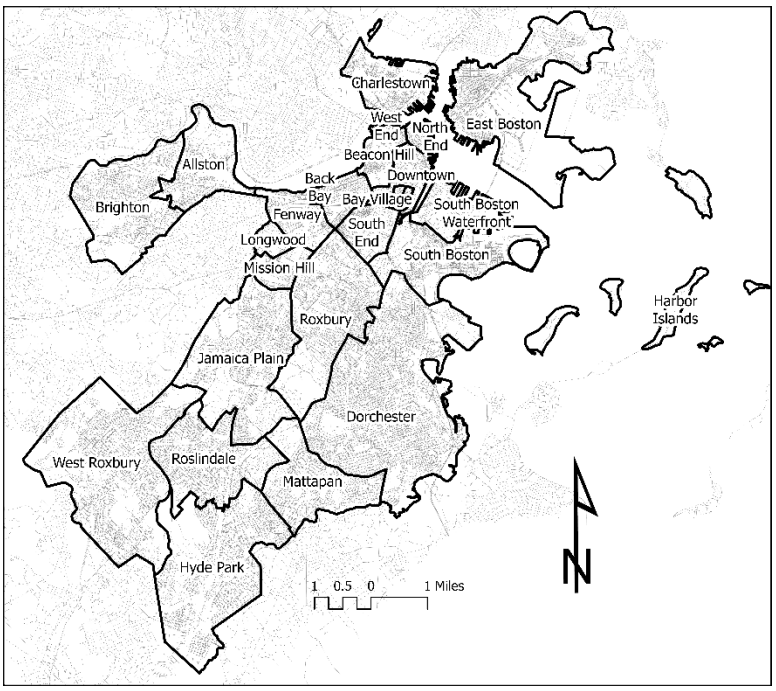

Figure 4 Names and spatial boundaries of all neighborhoods located within the City of Boston

3.1 RWH Systems Optimized for Maximized Life Cycle Cost and Energy Savings

Figure 5 presents the spatial distribution of the optimal tank sizes, life cycle cost, life cycle energy savings, and the percent demand met of RWH systems across Boston city when they are optimized for life cycle cost and life cycle energy, respectively. The average cost-optimized tank size is 3.25 m^3 (ranging from 0.04 ~ 17.7 m^3; Figure 5A). Larger tank sizes are generally correlated with higher life cycle cost savings (r=0.976; see the Supporting Information for correlation coefficients for all reported metrics). Installing cost-optimized RWH systems across the city will lead to end users losing an average of $33/year. This indicates a generally limited economic attractiveness of RWH systems. The life cycle costs of individual buildings range from -$182 to $388 per year (Figure 5B). Out of the 68,567 residential buildings in Boston, only 8,130 or 12% are able to achieve positive cost savings. These buildings can be characterized with relatively larger roof sizes and lawn areas per tenant, which allow more rainwater to be collected and used without extra pumping. Buildings with high life cycle costs are those with high building heights and tenant numbers but very limited lawn irrigation needs. This is because of their high pumping costs associated with

applying the collected rainwater for toilet flushing. Buildings that can yield positive cost savings are more common in the middle city such as the Jamaica Plain, Roxbury and Dorchester neighborhoods, while buildings with negative cost savings are more common in high-density communities in the downtown and its surrounding areas. However, high-density areas are often more prone to flooding risk, which can be mitigated through RWH systems. Hence, creating shared RWH systems amongst large apartment buildings with nearby parks or buildings with larger irrigation needs can potentially co-optimize both the cost of RWH systems and the reduction of flooding risk.

All cost-optimized RWH systems result in an increase in the life cycle energy consumption for providing water and wastewater services. The increase in life cycle energy ranges from 384 to 1,528 MJ per year with an average of 417 MJ/year (Figure 5C). This is largely due to the energy needed for constructing and implementing the RWH systems. The avoided pumping and treatment energy use at the DWTP and WWTP were found to offset only about 40 % of the embodied energy associated with the RWH systems over a 30-year time frame. Life cycle energy of the RWH systems across the city has a distinct spatial pattern as compared with that of life cycle cost (r=0.055). This is because, as compared to life cycle cost, life cycle energy is further influenced by a building's distance from the DWTP and its elevation. This finding indicates the potential importance of these spatial characteristics as well as the spatial RWH adoption patterns in determining the potential energy benefits. Overall, buildings located in the southern sub-urban areas and East Boston use relatively less energy due to their relatively higher elevations and larger lawn areas. Downtown areas such as Back Bay and South End have more buildings with very high energy use, mainly due their higher toilet flushing pumping need.

Cost-optimized RWH systems can meet an average of 21% of the flushing and lawn irrigation demand, with values for individual buildings range from 0.62 to 95 % (Figure 5D). These RWH systems combined save an average of 6.0 million m^3/year from the DWTP. Demand met is dependent on both the amount of rainwater that can be collected as well as the overall irrigation and toilet flushing demand. The spatial

distribution of percent demand met is relatively uniform across the city, except that the downtown area has the highest demand met in general.

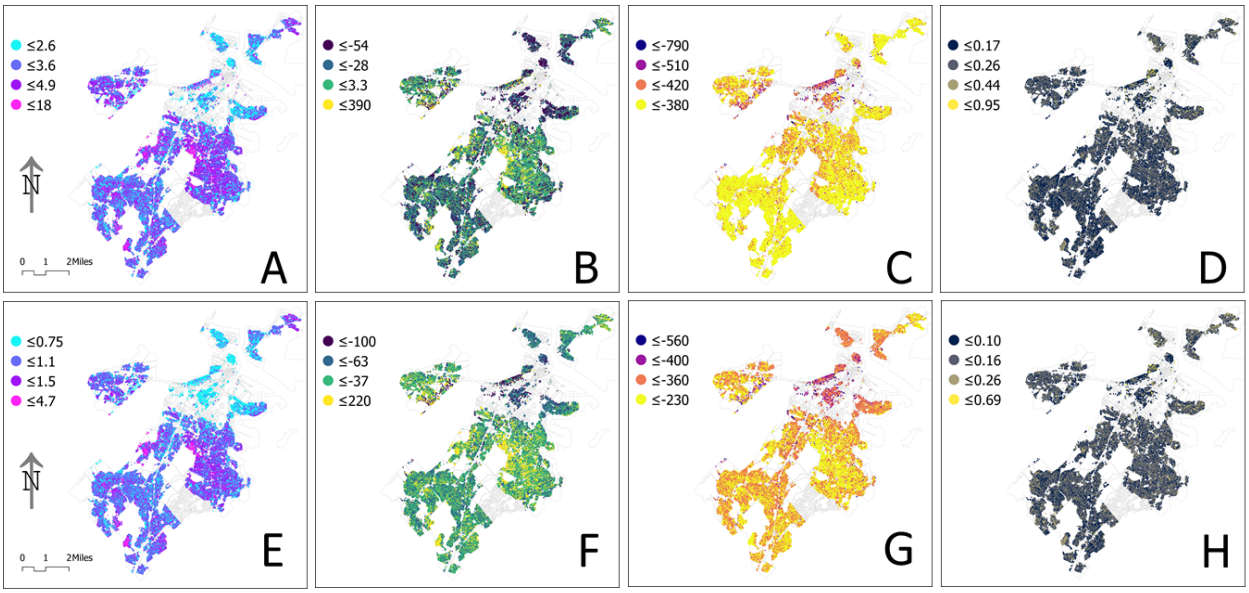

Figure 5 The spatial distribution of A) cost-optimized tank sizes (m^3); B) cost-optimized life cycle cost saving ($/year); C) cost-optimized life cycle energy saving (MJ/year); D) cost-optimized demand met (%); E) energy-optimized tank sizes (m^3); F) energy-optimized life cycle cost saving ($/year); G) energy-optimized life cycle energy saving (MJ/year); H) energy-optimized demand met (%) of residential rainwater harvesting (RWH) systems in the city of Boston.

The average energy-optimized tank size across the city is 0.94 m^3, with tank sizes for individual buildings range from 0.04 ~ 4.69 m^3 (Figure 5E). These tank sizes are generally much smaller compared with cost-optimized tank sizes, although they are highly correlated (r=0.908). The average size of the energy-optimized tanks is around 29% of the cost-optimized tank size. Smaller tank size is favored from an energy perspective because of the relatively more significant contribution of the construction and installation phase to the life cycle energy. Nevertheless, smaller tanks are less favorable from a stormwater management perspective.

Energy-optimized RWH systems will lead to an average loss of $57 per year for end users, with life cycle costs of individual buildings range from -$219 to $219 per year (Figure 5F). In general, energy optimization imposes a higher economic cost on end users. Only 670 buildings (around 1% of all buildings) are able to achieve positive cost savings. All buildings experience increased life cycle energy consumption after installing RWH systems, ranging from 231 to 929 MJ/year (Figure 5G). The average increase in life cycle energy is 362 MJ/year, which is slightly lower than the increase under cost optimization. Comparing the cost and energy optimization results, the cost efficiency of life cycle energy reduction is ($57/year-$33/year)/(417 MJ/year-362 MJ/year) = $0.44/MJ of primary energy. Considering the primary energy factor applied, this value can be further converted to a cost effectiveness of $0.27/kWh, which is higher than Boston's electricity price (USBLS 2020). This indicates a potential lack of attractiveness for adopting energy-optimized system sizes. Most of the buildings with the highest energy use under energy-optimization are located in the downtown area (Back Bay, Allston, and South End neighborhoods), where buildings can be characterized with larger height, higher occupancy, smaller lawn area per tenant, and longer distance from the DWTP. Buildings with lower life cycle energy consumption are generally located in the middle city, especially those with relatively longer distances from the DWTP and larger roof areas per tenant. In contrast, communities in the downtown and its surrounding areas have the highest life cycle energy consumption.

The energy-optimized RWH systems can only meet an average of 13% of the irrigation and toilet flushing demand, with individual buildings range from 0% - 69% (Figure 5H). These systems combined save an average of 3.8 million m^3/year from the DWTP. The spatial distribution of energy-optimized percent demand met is also relatively uniform across the city.

3.2 GWR Systems Optimized for Maximized Life Cycle Cost and Energy Savings

Figure 6 presents the spatial distribution of the optimal tank sizes, life cycle cost, life cycle energy savings, and the percent demand met of GWR systems across Boston city when they are optimized for life cycle

449 cost and life cycle energy, respectively. The average cost-optimized tank size is 2.35 m^3, with individual
450 building values range from 0.04 to 20.31 m^3 (Figure 6A).
451
452 All buildings installed with cost-optimized GWR systems can achieve positive cost savings, which range
453 from $52 to $19,351/year (Figure 6B). The average cost saving is $948/year. Unlike RWH systems, higher
454 cost savings are achieved in buildings with higher tenant number but not necessarily with big tanks, as such
455 systems produce a higher yield but relatively low construction cost. These buildings are generally located
456 in communities the downtown and its surrounding areas. In contrast, neighborhoods located in southern
457 sub-urban areas have the lowest cost saving.
458
459 Around 98% of the cost-optimized GWR systems can achieve energy savings with an average saving of
460 586 MJ/year. Actual energy saving of individual buildings range from -34,532 to 4,035 MJ/year (Figure
461 6C). The distribution of life cycle energy saving has a very different pattern as compared to the distribution
462 of life cycle cost saving (r=-0.108), indicating the important influences of spatial characteristics such as
463 elevation and distance from the DWTP. Neighborhoods located in the middle city perform the best from
464 the energy perspective, mainly due to generally lower building heights and longer distance from the DWTP.
465 Neighborhoods located in southern sub-urban areas have the lowest energy saving.
466
467 Cost-optimized GWR systems can meet 82% of the irrigation and toilet flushing demand on average, with
468 values for individual buildings range from 2 to 100% (Figure 6D). These GWR systems combined save an
469 average of 26.6 million m^3/year from the DWTP. Overall, the downtown area and the northern Boston have
470 the highest demand met while the southern sub-urban area has the lowest.

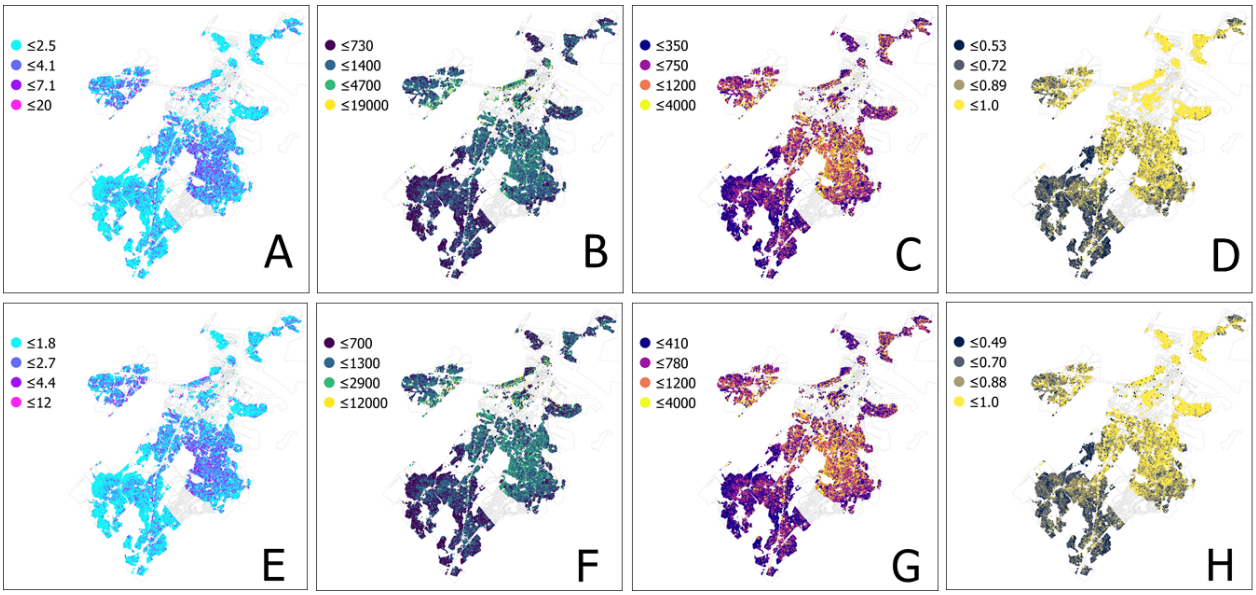

Figure 6 The spatial distribution A) cost-optimized tank sizes (m3); B) cost-optimized life cycle cost saving ($/year); C) cost-optimized life cycle energy saving (MJ/year); D) cost-optimized life cycle demand met (%); E) energy-optimized tank sizes (m3); F) energy-optimized life cycle cost saving ($/year); G) energy-optimized life cycle energy saving (MJ/year); H) energy-optimized demand met (%) of residential greywater recycling (GWR) systems in the city of Boston.

Energy-optimized GWR systems have smaller tank sizes compared with cost-optimized GWR systems. Energy-optimized tank sizes range from 0.03~11.74 m^3 with an average of 1.7 m^3 (Figure 6E). Energy-optimized tank sizes have a relatively high correlation with cost-optimized tank sizes (r=0.801). Energy-optimized tank sizes are also relatively indicative of GWR's life cycle cost saving (r=0.834) and life cycle energy saving (r=0.829).

Almost all the households (>99.9%) can achieve cost saving under energy optimization. The average cost saving is $909/year, with individual building values range from -$182 to $11,522/year (Figure 6F). Energy optimization only slightly reduces average cost saving by 6% as compared to cost optimization. This indicates the economic savings of GWR systems are not very sensitive to the optimization objectives,

488 although they result in significantly different GWR system sizes (38% difference) being installed. Similar
489 to cost optimization, the downtown area generally performs the best in terms of cost saving, while the
490 southern sub-urban area has the least cost saving.
491
492 About 98 % of the buildings can achieve positive energy saving. The average energy saving is 622 MJ/year,
493 with individual building savings range from -966 ~ 4,035 MJ/year (Figure 6G). Similarly, energy
494 optimization only resulted in a slight increase (4%) in the average energy saving as compared to cost
495 optimization. A cost efficiency of life cycle energy reduction can be calculated as ($948/year-
496 $909/year)/(622 MJ/year-586 MJ/year) = $1.08/MJ of primary energy, which is even more expensive
497 compared to the value calculated for RWH systems. This again indicates a low attractiveness for adopting
498 energy-optimized GWR system sizes as compared to cost-optimized system sizes. Unlike cost-
499 optimization, buildings with the highest life cycle saving are mainly located in the middle of the city as
500 compared to downtown area. Distance to the DWTP and elevation play a relatively small role here, as areas
501 with higher elevations are generally closer to the DWTP.
502
503 The average demand met of energy-optimized GWR systems is 81 %, with individual building values range
504 from 0~100 % (Figure 6H). These systems combined save an average of 25.5 million m^3/year from the
505 DWTP. The met demand throughout the city has a similar pattern under cost and energy optimizations.
506

507 **3.3 Comparison of the RWH with GWR systems**

508 Larger cost-optimized tank sizes are needed for the RWH systems than GWR systems to store and supply
509 more water and minimize the cost. However, the energy optimized tanks of the RWH systems are smaller
510 than the GWR systems, which is mainly due to GWR's more significant energy savings, resulting in the
511 system construction energy being less significant. While RWH systems can barely save any energy or
512 money, GWR system can provide both cost and energy savings for most of the buildings. Water supply
513 performance of GWR systems are also superior to RWH systems. The reason for this is because GWR

systems have a relatively constant daily greywater supply, while the RWH systems depend on intermittent rainfalls.

For RWH systems, buildings with larger roof areas and larger tank sizes in the middle of the city allows for a higher cost saving. However, for GWR systems, high occupancy buildings in the downtown area, not necessarily with big tanks are able to achieve higher cost saving. Larger tanks allow for more storage for rainwater in RWH systems, while higher occupancy allows for more tank refill in GWR systems. However, larger tank sizes are not favored from an energy perspective, because of their more significant construction and installation energy contributions to the life cycle energy. This effect is prominent in both RWH and GWR systems when they are being optimized for cost savings. However, when these systems are optimized for energy savings, the resulting life cycle cost and energy savings present a more identical spatial pattern. This indicates a potential tradeoff between the "individual good" (i.e., user cost) and the "common good" (i.e., energy saving on a city perspective), when users choose to adopt cost-optimized system sizes. Incentives might be developed to balance both the "individual good" and the "common good".

Spatially, the middle city area is generally good for both RWH and GWR system adoptions from both cost and energy perspectives. This is because the area has relatively dense population, higher building occupancy, but more single-family housing units with relatively larger roof area and higher irrigation demand. This area also has a relatively lower economic status with aged infrastructure systems as compared to other communities in Boston (LDEST 2020). Incentives might be provided to allow shared, combined RWH and GWR systems to be considered with infrastructure renovation efforts to maximize cost and energy benefits for the local communities. The southern sub-urban areas are the most suitable for installing RWH systems. This is because the area has relatively low population density, high elevation, and large lawn areas. Promotion of GWR systems needs to be avoided in these areas. The downtown and its surrounding areas are the most suitable for promoting GWR systems. This is because the area has the highest population density combined with more multi-family housing units. When taking stormwater

management into consideration, the downtown area can also benefit from combined RWH and GWR systems.

3.4 Sensitivity Analysis

Table 2 presents the sensitivity indices of the RWH and GWR's life cycle cost and energy savings when installed in an average household. The life cycle energy savings of the GWR and RWH systems were not highly sensitive to changes of most input variables, except when pumping efficiency is significantly reduced in the GWR system. The GWR life cycle energy is moderately sensitive to changes in the fixture rate and shower flow, as well as reductions in centralized system pumping efficiency, indicating the general importance of pumping energy and shower greywater supply in determining the GWR energy. The RWH life cycle energy is moderately sensitive to the tank embodied energy, indicating the importance of initial construction in determining the RWH energy. The GWR system's life cycle cost was highly sensitive to water and wastewater prices with a sensitivity index of 1.2. It is also moderately sensitive to the fixture rate. The RWH system's life cycle cost was highly sensitive to changes in the water price, the annual maintenance cost, and the reductions in the discount rate. This can be explained by the relatively significant maintenance cost contribution in the RWH system compared to the annual pumping cost.

Table 2 Absolute sensitivity index under input changes for the life cycle cost and energy savings associated with the RWH and the GWR systems when installed in a typical household in Boston

Absolute sensitivity index	GWR (life cycle cost saving)				GWR (life cycle energy saving)				RWH (life cycle cost saving)				RWH (life cycle energy saving)			
Input changes (%)	-50	-25	25	50	-50	-25	25	50	-50	-25	25	50	-50	-25	25	50
Discount rate	0.50	0.47	0.41	0.38					**1.03**	0.95	0.83	0.78				
Pump efficiency	0.01	0.01	0.00	0.00	0.95	0.64	0.38	0.32	0.06	0.04	0.02	0.02	0.31	0.20	0.12	0.10
Electricity price	0.01	0.01	0.01	0.01					0.03	0.03	0.03	0.03				
Irrigation efficiency	0.00	0.00	0.00	0.00	0.08	0.07	0.06	0.06	0.00	0.00	0.00	0.00	0.00	0.01	0.00	0.00
Laundry flow	0.10	0.10	0.10	0.10	0.19	0.19	0.19	0.19								
Sink flow	0.12	0.12	0.12	0.12	0.24	0.24	0.24	0.23								
Floor height	0.00	0.00	0.00	0.00	0.14	0.14	0.14	0.14								
Fixture rate	0.61	0.58	0.56	0.51	0.88	0.82	0.81	0.73								
Water (and wastewater) price	**1.16**	**1.16**	**1.16**	**1.16**					**2.36**	**2.36**	**2.36**	**2.36**				

Plant factor	0.02	0.00	0.00	0.00	0.12	0.08	0.05	0.05	0.00	0.00	0.00	0.00	0.00	0.00	0.01	0.01
Shower flow	0.36	0.35	0.34	0.31	0.69	0.69	0.66	0.60								
Number of tenants per fixture	0.00	0.00	0.00	0.00	0.01	0.00	0.00	0.00	0.02	0.00	0.00	0.00	0.01	0.00	0.00	0.00
Potential evapotranspiration	0.02	0.00	0.00	0.00	0.12	0.08	0.05	0.05	0.00	0.00	0.00	0.00	0.01	0.01	0.00	0.00
Friction loss coefficient					0.34	0.34	0.34	0.34					0.09	0.09	0.09	0.09
Central pumping efficiency					0.57	0.38	0.23	0.22					0.15	0.10	0.06	0.06
Operation pressure					0.02	0.02	0.02	0.02					0.01	0.01	0.01	0.01
Maintenance energy intensity					0.30	0.30	0.30	0.30					0.36	0.36	0.36	0.36
Pump embodied energy					0.18	0.18	0.18	0.18					0.22	0.22	0.22	0.22
Tank embodied energy					0.38	0.38	0.38	0.38					0.46	0.46	0.46	0.46
Installation energy intensity					0.14	0.14	0.14	0.14					0.17	0.17	0.17	0.17
Velocity in pipeline					0.00	0.00	0.00	0.00					0.00	0.00	0.00	0.00
Adj factor					0.28	0.28	0.28	0.28					0.07	0.07	0.00	0.00
Installation cost	0.02	0.02	0.02	0.02	0.14	0.14	0.14	0.14	0.35	0.35	0.35	0.35	0.17	0.17	0.17	0.17
Annual maintenance cost	0.08	0.08	0.08	0.08	0.30	0.30	0.30	0.30	**1.83**	**1.83**	**1.83**	**1.83**	0.36	0.36	0.36	0.36

4. Conclusion

This study investigated the cost and energy implications of decentralized, household RWH and GWR system adoptions from a spatial perspective. Particularly, we investigated the spatial distributions of life cycle cost, life cycle energy, and percent demand met of these two systems under cost- and energy-optimized system sizes. Simulations were conducted for each individual residential household in the city of Boston. The results showed that RWH systems can only allow 12% or less of the residential buildings in the city to achieve positive cost savings no matter under cost- or energy-optimization. Installation of these RWH systems will increase the overall energy use by an average of 362-417 MJ/year. The average percent demand met that can be provided through RWH system installations is around 13-21% of the total toilet flushing and irrigation demand. GWR systems are able to achieve much higher cost and energy savings and percent demand met as compared with RWH systems. An average life cycle cost saving of $909-948/year and an average life cycle energy saving of 586-622 MJ/year can be achieved via installing cost- or energy-optimized GWR systems. Meanwhile, averaged percent demand met is around 81-82% of the total toilet flushing and irrigation demand. We also found that spatial characteristics such as a building's

elevation and its distance from the DWTP can have a notable effect on the life cycle energy savings of both the RWH and the GWR systems, which aligns with findings from Kavvada et al. (2016).

There is also a tradeoff between the "individual good" (i.e., user life cycle cost) and the "common good" (i.e., life cycle energy saving on a city perspective) in both RWH and GWR systems when the tank sizes are optimized for cost savings. Incentives might be provided to nudge individual users' behaviors toward the common good. For instance, the middle city area is generally good for both RWH and GWR system adoptions from both cost and energy perspectives. This area is also one of the oldest areas in Boston with relatively low economic income. Hence, incentives might be provided to foster the consideration of shared, combined RWH and GWR systems with infrastructure renovation efforts to allow maximized cost and energy benefits for the local communities. On the other hand, the southern sub-urban areas are generally the most suitable for installing RWH systems, while the downtown and its surrounding areas are generally the most suitable for promoting GWR systems. When taking stormwater management into consideration, the downtown area can also benefit from combined RWH and GWR systems as well as shared systems with local parks or other buildings with larger irrigation demands.

Lastly, a changing economy or environment could also impact the economic and energy feasibility of GWR and RWH, especially in areas with existing water shortage or scarcity. If the utility prices of water and wastewater increase, homeowners could potentially see higher cost savings with the use of water that is recycled or reused. Water and wastewater treatment could also require more energy, as emerging pollutants are regulated and new energy-intensive steps need to be added to the treatment train, all of which can potentially lead to an increased attractiveness of RWH or GWR systems. The modeling framework presented in this study can be generalized to assist with incentive design and planning of decentralized water systems.

Acknowledgements

We acknowledge the National Science Foundation's support via a CBET award (#1706143) and a CRISP Type I Award (#1638334). The views, findings, and conclusions expressed in this study are those of the authors and do not necessarily reflect the views of the National Science Foundation. We would also like to thank Soheil Gharatappeh for assisting with high performance computing.

References

Abbas, A.I., Qandil, M.D., Al-Haddad, M.R., Saravani, M.S. and Amano, R.S. (2018) Utilization of Hydro-Turbines in Wastewater Treatment Plants (WWTPs), pp. V001T001A003-V001T001A003, American Society of Mechanical Engineers.

Angrill, S., Farreny, R., Gasol, C.M., Gabarrell, X., Viñolas, B., Josa, A. and Rieradevall, J. (2012) Environmental analysis of rainwater harvesting infrastructures in diffuse and compact urban models of Mediterranean climate. The International Journal of Life Cycle Assessment 17(1), 25-42.

ASCE (2017) Water Infrastructure | ASCE's 2017 Infrastructure Report Card. Engineers, A.S.o.C. (ed), https://www.infrastructurereportcard.org/cat-item/drinking-water/.

AWWA (2001) Dawn of the Replacement Era - Reinvesting in Drinking Water Infrastructure, American Water Works Association.

Bowen, J.L., Baillie, C.J., Grabowski, J.H., Hughes, A.R., Scyphers, S.B., Gilbert, K.R., Gorney, S.G., Slevin, J. and Geigley, K.A. (2019) Boston Harbor, Boston, Massachusetts, USA: Transformation from 'the harbor of shame' to a vibrant coastal resource. Regional Studies in Marine Science 25, 100482.

Brent, R.P. (1971) An algorithm with guaranteed convergence for finding a zero of a function. The Computer Journal 14(4), 422-425.

Brière, F.G. (2014) Drinking-water distribution, sewage, and rainfall collection, Presses inter Polytechnique.

BWSC (2019) Boston Water and Sewer Rates, Boston Water and Sewer Commission, https://www.bwsc.org/residential-customers/rates.

CMU (2018) Economic Input-Output Life Cycle Assessment, Carnegie Mellon University, http://www.eiolca.net.

COB (2019) Boston Maps Open Data Geospatial Datasets, http://bostonopendata-boston.opendata.arcgis.com.

630 Dieter, C.A., Maupin, M.A., Caldwell, R.R., Harris, M.A., Ivahnenko, T.I., Lovelace, J.K., Barber, N.L.
631 and Linsey, K.S. (2018) Estimated use of water in the United States in 2015, US Geological
632 Survey.
633 Dixon, A., Butler, D., Fewkes, A. and Robinson, M. (2000) Measurement and modelling of quality
634 changes in stored untreated grey water. Urban Water 1(4), 293-306.
635 EPA (2003) Water efficient irrigation study, Saving water partnership.
636 Ghimire, S.R., Johnston, J.M., Ingwersen, W.W. and Hawkins, T.R. (2014) Life Cycle Assessment of
637 Domestic and Agricultural Rainwater Harvesting Systems. Environmental science & technology
638 48(7), 4069-4077.
639 Ghorbanian, V., Karney, B. and Guo, Y. (2016) Pressure Standards in Water Distribution Systems:
640 Reflection on Current Practice with Consideration of Some Unresolved Issues. Journal of Water
641 Resources Planning and Management 142(8), 04016023.
642 Godskesen, B., Zambrano, K., Trautner, A., Johansen, N.-B., Thiesson, L., Andersen, L., Clauson-Kaas,
643 J., Neidel, T., Rygaard, M. and Kløverpris, N. (2011) Life cycle assessment of three water
644 systems in Copenhagen–a management tool of the future. Water Science and Technology 63(3),
645 565-572.
646 Gwenzi, W., Dunjana, N., Pisa, C., Tauro, T. and Nyamadzawo, G. (2015) Water quality and public
647 health risks associated with roof rainwater harvesting systems for potable supply: Review and
648 perspectives. Sustainability of Water Quality and Ecology 6, 107-118.
649 Hamilton, K.A., Ahmed, W., Toze, S. and Haas, C.N. (2017) Human health risks for Legionella and
650 Mycobacterium avium complex (MAC) from potable and non-potable uses of roof-harvested
651 rainwater. Water research 119, 288-303.
652 Hanson, L.S., Vogel, R.M., Kirshen, P. and Shanahan, P. (2009) Generalized Storage-Reliability-Yield
653 Equations for Rainwater Harvesting Systems, American Society of Civil Engineers.
654 Hargreaves, A.J., Farmani, R., Ward, S. and Butler, D. (2019) Modelling the future impacts of urban
655 spatial planning on the viability of alternative water supply. Water research 162, 200-213.

656 Hunter, P.R., MacDonald, A.M. and Carter, R.C. (2010) Water supply and health. PLoS medicine 7(11),
657 e1000361-e1000361.
658 INTEWA (2020) Pumps, operation and rainwater units, INTEWA Wiki,
659 https://wiki.intewa.net/index.php/Pumpen,_Betriebs-
660 _und_Regenwasserwerke/en#Definition_of_the_simultaneity_factor.
661 Jeong, H., Broesicke, O.A., Drew, B., Li, D. and Crittenden, J.C. (2016) Life cycle assessment of low
662 impact development technologies combined with conventional centralized water systems for the
663 City of Atlanta, Georgia. Frontiers of Environmental Science & Engineering 10(6), 1.
664 JFW (2014) Optimizing the structure and scale of urban water infrastructure: integrating distributed
665 systems. Wingspread, T.J.F.a. (ed).
666 Jones M, H.W. (2020) Choosing a Pump for Rainwater Harvesting, North Carolina Cooperative
667 Extension Service,
668 https://www.ctahr.hawaii.edu/hawaiirain/Library/Guides&Manuals/NC_Choosing-a-
669 Pump4RWH2006.pdf.
670 Kavvada, O., Horvath, A., Stokes-Draut, J.R., Hendrickson, T.P., Eisenstein, W.A. and Nelson, K.L.
671 (2016) Assessing location and scale of urban nonpotable water reuse systems for life-cycle
672 energy consumption and greenhouse gas emissions. Environmental science & technology 50(24),
673 13184-13194.
674 Khalkhali, M. and Mo, W. (2020) The energy implication of climate change on urban wastewater
675 systems. Journal of Cleaner Production, 121905.
676 Khalkhali, M., Westphal, K. and Mo, W. (2018) The water-energy nexus at water supply and its
677 implications on the integrated water and energy management. Science of the Total Environment
678 636, 1257-1267.
679 Kjelgren, R., Beeson, R.C., Pittenger, D.P. and Montague, T. (2016) Simplified landscape irrigation
680 demand estimation: slide rules. Applied Engineering in Agriculture 32(4), 363-378.

LDEST (2020) Oldest parts of Boston. LDEST.ORG (ed), https://www.oldest.org/geography/parts-of-boston/.

López Zavala, M., Castillo Vega, R. and López Miranda, R. (2016) Potential of Rainwater Harvesting and Greywater Reuse for Water Consumption Reduction and Wastewater Minimization. Water 8(6), 264.

Maps, B. (2019) Analyze Boston. Boston, A. (ed), Open Data Commons Public Domain Dedication and License (PDDL), Boston Maps.

Memon, F., Zheng, Z., Butler, D., Shirley-Smith, C., Lui, S., Makropoulos, C. and Avery, L. (2007) Life cycle impact assessment of greywater recycling technologies for new developments. Environmental monitoring and assessment 129(1-3), 27.

Mo, W., Wang, H. and Jacobs, J.M. (2016) Understanding the influence of climate change on the embodied energy of water supply. Water research 95, 220-229.

Morales-Pinzón, T., Rieradevall, J., Gasol, C.M. and Gabarrell, X. (2015) Modelling for economic cost and environmental analysis of rainwater harvesting systems. Journal of Cleaner Production 87, 613-626.

MWRA (2006) Water system master plan, Massachusetts Water Resources Authority, Massachusetts Water Resources Authority.

Newman, J., Dandy, G. and Maier, H. (2014a) Multiobjective optimization of cluster-scale urban water systems investigating alternative water sources and level of decentralization. Water Resources Research 50(10), 7915-7938.

Newman, J.P., Dandy, G.C. and Maier, H.R. (2014b) Multiobjective optimization of cluster-scale urban water systems investigating alternative water sources and level of decentralization. Water Resources Research 50(10), 7915-7938.

NOAA (2019) National Centers for Environmental Information: Climate Data Online, National Oceanic and Atmostpheric Association, https://www.ncdc.noaa.gov/cdo-web/.

706 NRCC (2020) Potential evapotranspiration for selected locations, Northeast regional climate center
707 http://www.nrcc.cornell.edu/wxstation/pet/pet.html

708 NRCNA (2006) Drinking Water Distribution Systems: Assessing and Reducing Risk, National Research
709 Council of the National Academies, https://www.nap.edu/read/11728/chapter/1.
710 Romero, C.C. and Dukes, M.D. (2008) Turfgrass Crop Coefficients in the US, Irrigation Association.
711 Song, C., Omalley, A., Roy, S.G., Barber, B.L., Zydlewski, J. and Mo, W. (2019) Managing dams for
712 energy and fish tradeoffs: What does a win-win solution take? Science of the Total Environment
713 669, 833-843.
714 USBLS (2020) Consumer price index, U.S. Bureau of Labor Statistics, https://www.bls.gov/cpi/.
715 USCB (2019) American Fact Finder, U.S. Census Bureau,
716 https://factfinder.census.gov/faces/nav/jsf/pages/index.xhtml.
717 USEPA (2013). Agency, U.S.E.P. (ed), United States Environmental Protection Agency.
718 USGS (2019) USGS Domestic Water Use, States Geological Survey, https://www.usgs.gov/mission-
719 areas/water-resources/science/domestic-water-use?qt-science_center_objects=0#qt-
720 science_center_objectsUnited
721 Wang, R. and Zimmerman, J.B. (2015) Economic and environmental assessment of office building
722 rainwater harvesting systems in various US cities. Environmental science & technology 49(3),
723 1768-1778.
724 Wanjiru, E. and Xia, X. (2017) Optimal energy-water management in urban residential buildings through
725 grey water recycling. Sustainable cities and society 32, 654-668.
726 Ward, S., Memon, F.A. and Butler, D. (2012) Performance of a large building rainwater harvesting
727 system. Water research 46(16), 5127-5134.
728 WERF (2009) Advances in water research. Foundation, W.R. (ed), The water research foundation,
729 https://www.werf.org/.

730